MARLEY

RADIATIVE TRANSFER LECTURES

by Jim Pollack

II. INTERACTION OF LIGHT WITH PARTICLES

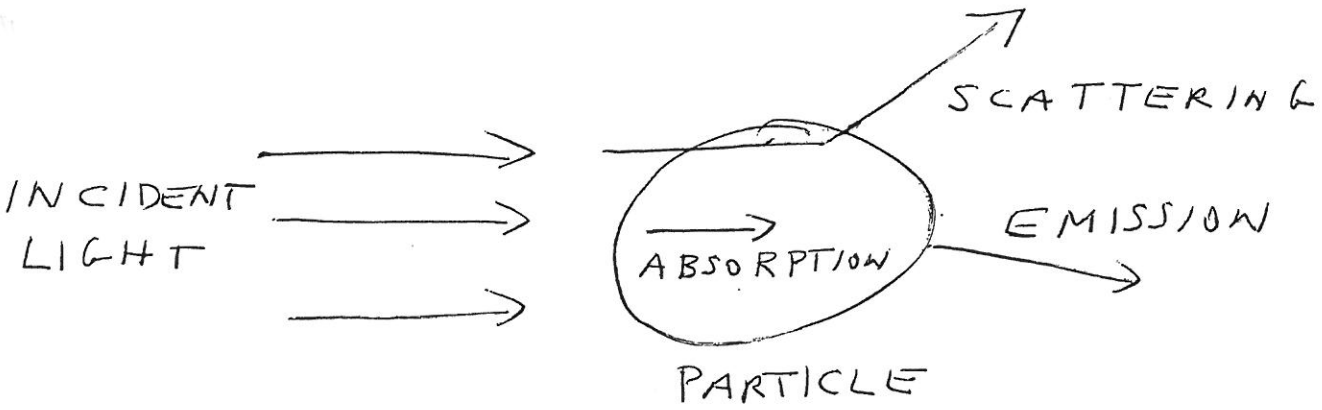

BASIC DEFINITIONS

PROJECTED GEOMETRIC CROSS SECTION

$$\sigma_{geo} = \pi a^2 \leftarrow \text{RADIUS}$$

TOTAL EXTINCTION (= SCATTERING + ABS.) X SECTION

$$\sigma_{ext} = Q_{ext}\, \sigma_{geo}$$

Q_{ext} ↑ EXTINCTION EFFICIENCY

SCATTERING X SECTION

$$\sigma_{scat} = Q_{scat}\, \sigma_{geo}$$

Q_{scat} ↑ scattering efficiency

ABSORPTION X SECTION

$$\sigma_{abs} = Q_{abs}\, \sigma_{geo}$$

Q_{abs} ↑ absorption efficiency

EMISSION X SECTION

$$\sigma_{emis} = \sigma_{abs}$$

SINGLE SCATTERING ALBEDO

(RATIO OF SCATTERING TO EXTINCTION)

$$\tilde{\omega}_0 = \frac{\sigma_{scat}}{\sigma_{scat} + \sigma_{abs}} = \frac{Q_{scat}}{Q_{ext}}$$

SINGLE SCATTERING PHASE FUNCTION -

PROBABILITY OF LIGHT BEING SCATTERED AT AN ANGLE Θ

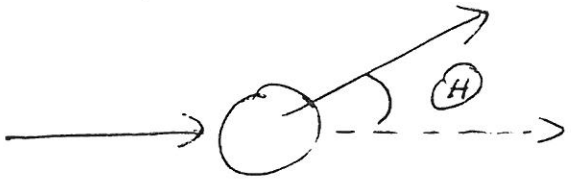

$\Theta = 0^\circ \rightarrow$ SAME DIRECTION AS INCIDENT LIGHT WAS TRAVELING, IE NO CHANGE OF DIRECTION

NORMALIZATION CONDITION ON PHASE FUNCTION, $P(\Theta)$

$$\int \frac{P(\Theta)\, d\Omega}{4\pi} = \text{[illegible]}$$

(solid ∠)

$$\int_0^{\pi} \int_0^{2\pi} P(\Theta) \sin(\Theta)\, d\phi\, d(\Theta)$$

$$= \frac{1}{2} \int_{-1}^{1} P(\mu)\, d\mu = 1$$

$$\mu = \cos(\Theta)$$

EXAMPLES OF PHASE FUNCTIONS:

ISOTROPIC (EQUAL PROBABILITY OF BEING SCATTERED INTO ANY SOLID Δ)

$$P_{ISO} = 1$$

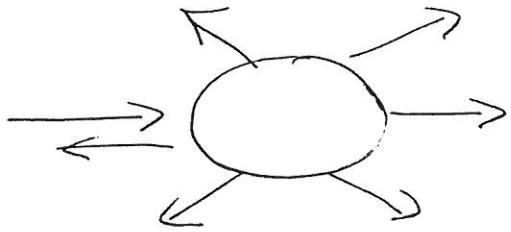

RAYLEIGH (PREFERENTIAL BACK & FORWARD SCATTERING)

$$P_{RAY} = \frac{3}{4}\left(1 + \cos^2 \Theta\right)$$

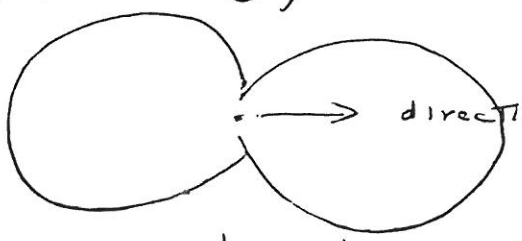

polar diagram

HENYEY GREENSTEIN

$$P_{HG} = \frac{1 - g^2}{\left(1 + g^2 - 2g\cos(\Theta)\right)^{3/2}}$$

ex. $g = 0 \rightarrow$ ISOTROPIC

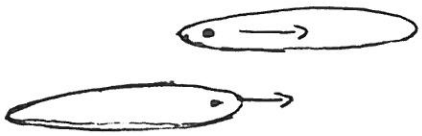

$g \rightarrow 1$ completely forward

$g \rightarrow -1$ completely backward

Legendre polynomial

$$P_{HG} = \sum_{l=0}^{\infty} (2l+1) g^l P_l(\cos(\Theta))$$

Double Henyey–Greenstein

(peaks in both forward ($\Theta = 0°$) & backwards directions ($\Theta = 180°$)

$$P_{DHG} = b\, P_{HG}(\cos(\Theta), g_1) + (1-b)\, P_{HG}(\cos(\Theta), g_2)$$

$$g_1 > 0, \quad g_2 < 0$$

VERY SMALL PARTICLES
(RAYLEIGH SCATTERING)

REQUIREMENT:

PHASE SHIFT ACROSS PARTICLE IS SMALL

$$\frac{2\pi a}{\lambda_0} |m_c| \equiv x |m_c| << 1$$

(2π IS PHASE CHANGE IN DISTANCE λ_0

λ_0 = WAVELENGTH IN VACUUM

m_c = COMPLEX INDEX OF REFRACTION

$= m_r + i m_i$

(m_r: real index; m_i: imaginary index)

→ PHASE OF INCIDENT E&M WAVE CONSTANT ACROSS PARTICLE →

~~PARTICLE REGARDED AS A DIPOLE~~

INDUCE DIPOLE MOMENT → EMITTED (ie SCATTERED) E+M WAVE

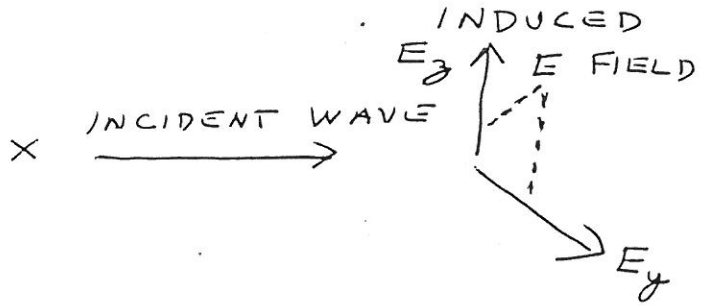

IN DIRECTION x BOTH E_x AND E_y CONTRIBUTE TO SCATTERED LIGHT

IN DIRECTION y (or z) ONLY E_z (or E_y) CONTRIBUTE

HENCE :

- p TWICE AS BIG AT $\Theta = 0$ & $180°$ AS p AT $\Theta = 90°$
- 100% POLARIZATION (LINEAR) AT $\Theta = 90°$
  0% AT $\Theta = 0$ & $180°$

KEY PROPERTIES OF SMALL PARTICLES

$$p(\Theta) = p_{RAY} = \frac{3}{4}(1 + \cos^2\Theta)$$

$\int_0^{\pi} \cos\Theta \, d\Theta \sim \int_0^{\pi} \sin\Theta \, d\Theta = \pi$ $\quad \langle \cos\Theta \rangle = 0$

$$\text{LINEAR POLARIZATION} = \frac{(1 - \cos^2\Theta)}{(1 + \cos^2\Theta)}$$

$$Q_{scat} = \frac{8}{3} x^4 \left| \frac{m_c^2 - 1}{m_c^2 + 2} \right|$$

$$Q_{abs} = 4x \, Im\left(\frac{m_c^2 - 1}{m_c^2 + 2} \right)$$

($|m_c| = (m_c * \tilde{m}_c)^{1/2}$, m_c = complex #, $\tilde{m}_c$ = [illegible] - COMPLEX CONJUGATE)

IMPLICATIONS

(1) $\sigma_{scat} \sim V^2$, $\sigma_{abs} \sim V$

(V = particle volume ~ # molecules)

(2) As $x \to 0$ $\quad Q_{scat} << Q_{abs}$

(3) $\sigma_{scat} \sim \lambda^{-4}$

$\longrightarrow$ SKY IS BLUE !

(WHEN ONLY AIR MOLECULES)

VERY BIG PARTICLES

CONDITION

$$X >> 1$$

HOW BIG IS BIG?

X SECTIONS : $X \gtrsim 10$

PHASE FUNCTIONS*: $X \gtrsim 500 - 1000$

POLARIZATION : $X \gtrsim 500 - 1000$

* FOR $\textcircled{H} \geq 60^\circ$

MUCH SMALLER X FOR $\textcircled{H} \leq 60^\circ$

PROCEDURE

— CLASSICAL DIFFRACTION THEORY

\+ — GEOMETRIC OPTICS OK

● USE RAY TRACING:

FOR EACH ORIENTATION

TRACE ALL RAYS THAT

INTERSECT THE SURFACE

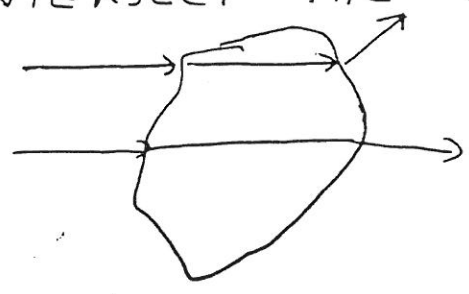

PHASE FUNCTION

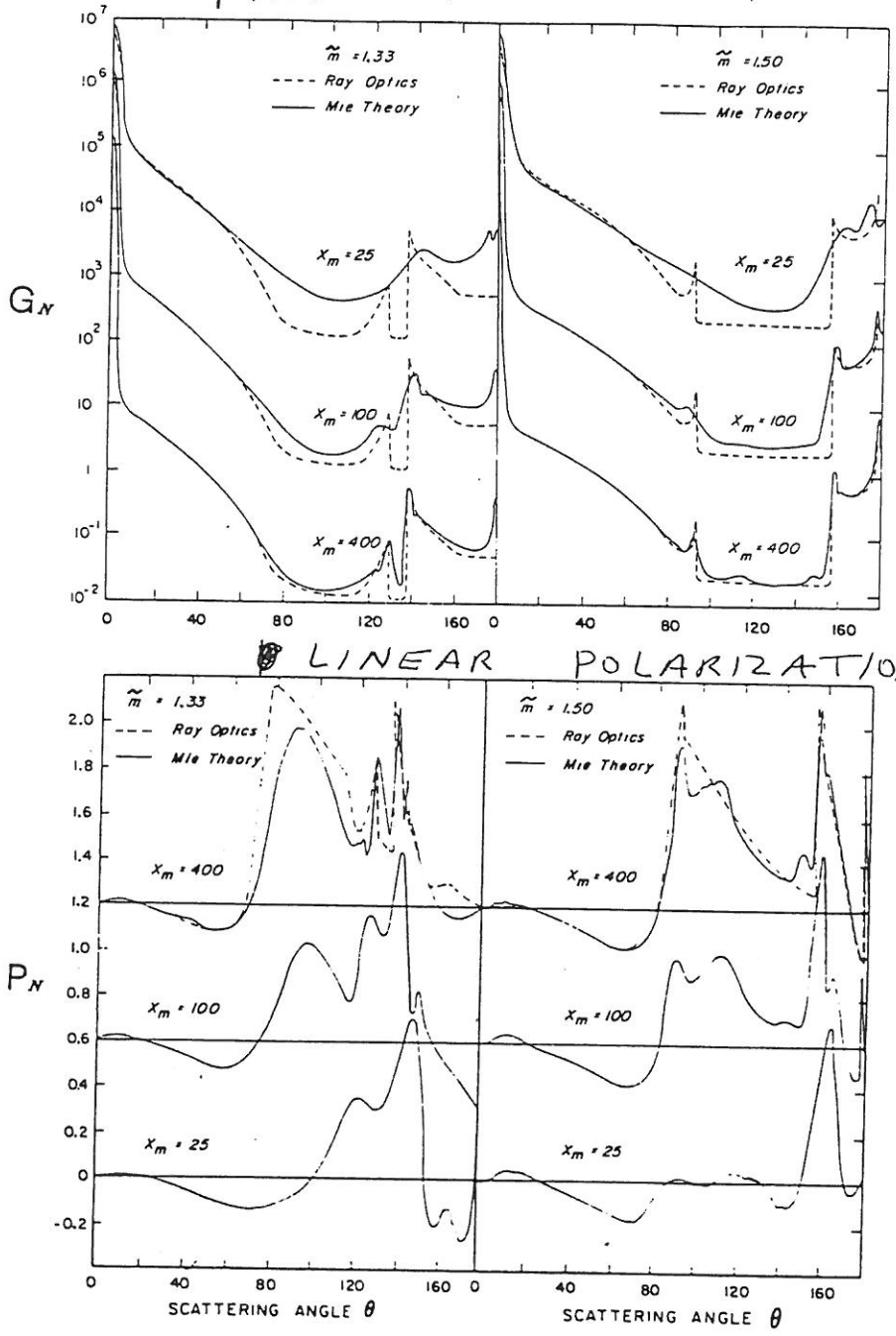

FIG. 7.15. Comparison between geometric optics and Mie theory. The phase function (G_N, upper figure) and polarization (P_N, lower figure) are for single scattering of unpolarized light by spheres. Results are shown for two real refractive indices and three values of x_m, which is the effective size parameter. After Hansen and Travis (1974).

EXTINCTION

I

S

FIG. 7.16. Formation of the glo
After Nussenzveig (1979).

$$g = \frac{\int [($$

Using (7.66), we can expre

$$g = \frac{4}{x^2 Q_s} \sum_{n=1}^{\infty} \frac{n(n+2)}{n+1} \mathcal{R}($$

For isotropic and Rayleigl
according as the particle
backward direction. a is un
unity for complex $\tilde{m}$. Nume
7.17 and 7.18, respectively.
approximation for cloud dr
($x = 1000$) can be quite da
behavior of a as $x \to \infty$ in F
metallic sphere is totally ref

It is now possible to c
spheres with size paramete
reveal how to recover analy
Recent work indicates that

The series in (7.66) are

RESULTS

$$\sigma_{geo} = \frac{1}{4} A_{surf}$$

(A_{surf}: surface area)

(if particle is randomly oriented + NO reentrants )

$$Q_{EXT} = 2$$

~~DEFRACT~~ DIFFRACTION + GEOMETRK OPTICS

($\sigma_{dif} = \sigma_{geo}$)

$$Q_{abs} \simeq (1 - \bar{R}_{EXT}) \exp(-k\bar{l})$$

($\bar{R}_{EXT}$ = Average amount of light externally reflected)

k = absorption coefficient/length

$\bar{l}$ = average path length thru particle)

$$k \equiv \frac{4\pi n_i}{\lambda}$$

$$\rightarrow k\bar{l} \simeq f \times$$

~~f = fac~~

f = factor $\cong$ several

COMMENTS:

(1) IF $x >>> 1$,
DIFFRACTION ALL AT VERY SMALL (H) → CAN BE NEGLECTED

(2) $\sigma_{ext} \sim A_{surf} \neq V$

RAY TRACING PHASE FUNCTIONS

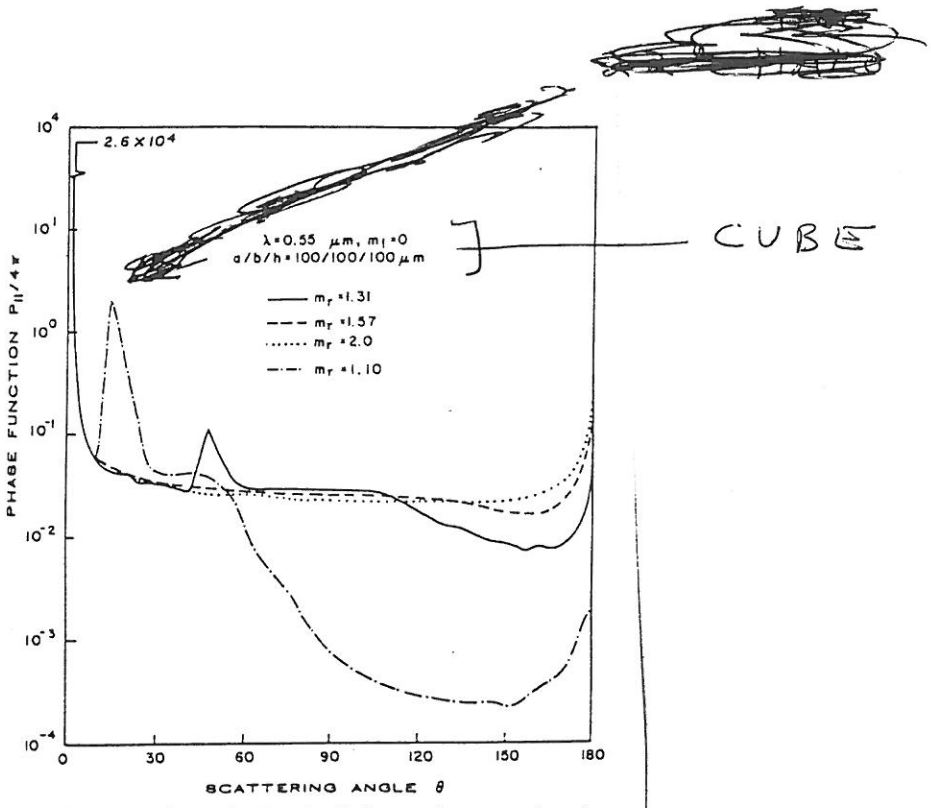

Fig. 3. Effects of the real refractive index on the scattering phase function for randomly oriented cubes as a function of the scattering angle.

GET RESONANT FEATURES WHEN $m_r < \sqrt{2}$
(∆ of minimum deviation)

EXAMPLE—
22° ICE HALO
(MOON + CIRRUS CLOUDS)
HEXAGONAL SHAPE PARTICLES

MIE THEORY

CONDITIONS:

- SPHERICAL PARTICLES
- ANY X (BUT COMPUTER TIME INCREASES AS X ↑)

WHAT

- EXACT SOLUTION OF MAXWELL'S EQUATIONS
- EASY TO SPECIFY BOUNDARY CONDITIONS
- USE ASSOCIATED LEGENDRE POLYNOMIALS TO GET "ANALYTICAL SOLUTION" → SERIES EXPANSION OF "AMPLITUDE FUNCTIONS" ($S_1(\theta)$ AND $S_2(\theta)$)

$$\text{INTENSITY} \sim |S_1|^2 + |S_2|^2$$

$$\text{POLARIZATION (LINEAR)} = \frac{|S_2|^2 - |S_1|^2}{|S_2|^2 + |S_1|^2}$$

MIE EQUATIONS

$$S_1(\theta) = \sum_{n=1}^{\infty} \frac{2n+1}{n(n+1)} [a_n \pi_n(\cos\theta) + b_n \tau_n(\cos\theta)],$$

$$S_2(\theta) = \sum_{n=1}^{\infty} \frac{2n+1}{n(n+1)} [b_n \pi_n(\cos\theta) + a_n \tau_n(\cos\theta)], \tag{7.66}$$

where

$$\pi_n(\cos\theta) = \frac{1}{\sin\theta} P_n^1(\cos\theta),$$

$$\tau_n(\cos\theta) = \frac{d}{d\theta} P_n^1(\cos\theta),$$

P_n^1 is an associated Legendre polynomial, and the coefficients a_n and b_n are given by

$$a_n = \frac{\psi_n'(\tilde{m}x)\psi_n(x) - \tilde{m}\psi_n(\tilde{m}x)\psi_n'(x)}{\psi_n'(\tilde{m}x)\zeta_n(x) - \tilde{m}\psi_n(\tilde{m}x)\zeta_n'(x)},$$

$$b_n = \frac{\tilde{m}\psi_n'(\tilde{m}x)\psi_n(x) - \psi_n(\tilde{m}x)\psi_n'(x)}{\tilde{m}\psi_n'(\tilde{m}x)\zeta_n(x) - \psi_n(\tilde{m}x)\zeta_n'(x)},$$

where

$$\psi_n(x) = (\tfrac{1}{2}\pi x)^{1/2} J_{n+1/2}(x),$$

$$\zeta_n(x) = (\tfrac{1}{2}\pi x)^{1/2} H_{n+1/2}^{(2)}(x),$$

are Riccati–Bessel functions and $J_{n+1/2}$ and $H_{n+1/2}^{(2)}$ are spherical Bessel functions. The Bessel functions have zeros that increase in number with the size of the argument, with the result that S_1 and S_2 can change rapidly for very small variations of x.

If extinction and scattering efficiencies alone are required these can be obtained from the expressions

$$Q_e = \frac{2}{x^2} \sum_{n=1}^{\infty} (2n+1)(a_n + b_n),$$

$$Q_s = \frac{2}{x^2} \sum_{n=1}^{\infty} (2n+1)(|a_n|^2 + |b_n|^2). \tag{7.67}$$

Q_{SCAT} VS $X\ (= 2\pi a/\lambda)$

ONLY ONE SIZE ($b = 0$)

VS AVERAGED OVER A SIZE DISTRIBUTION OF VARYING WIDTHS, b

DIFFERENTIAL (PARTICLE − AIR) PHASE SHIFT ACROSS PARTICLE

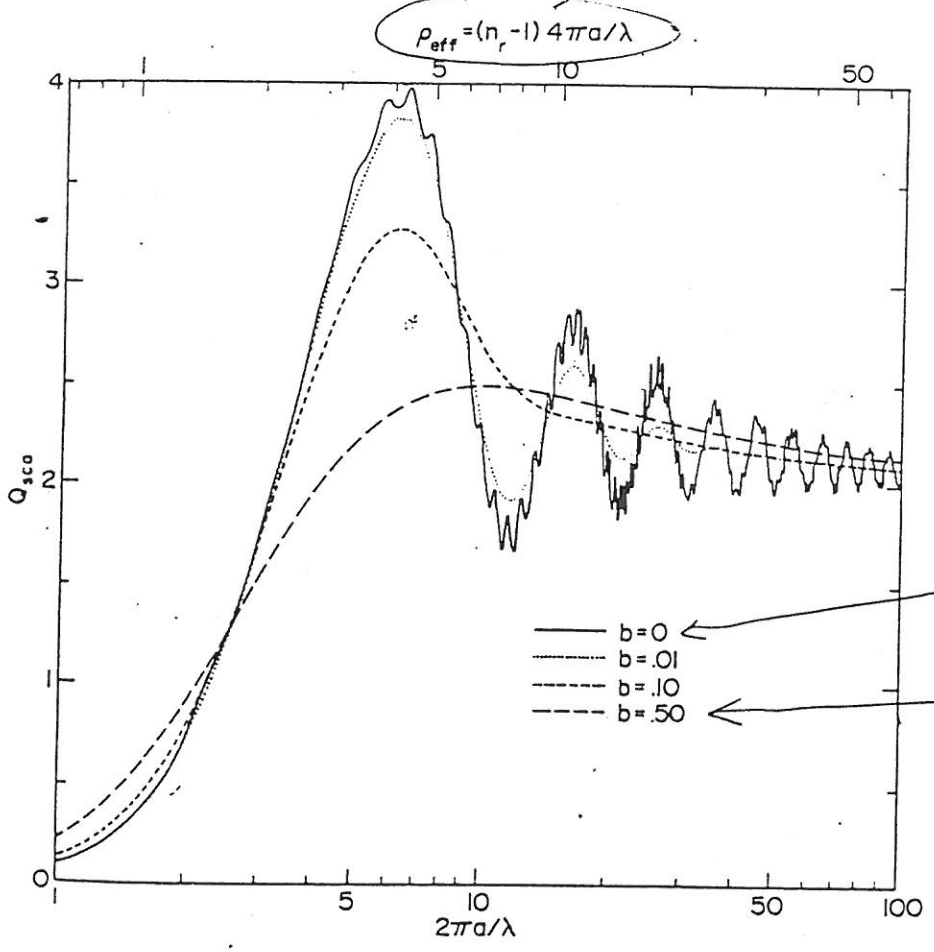

ONE SIZE

VERY BROAD SIZE DISTRIBUTION

Fig. 8. Efficiency factor for scattering, Q_{sca}, as a function of the effective size parameter, $2\pi a/\lambda$. The standard size distribution (2.56) was used with four values of the effective variance b. For the case $b = 0$, $2\pi a/\lambda = 2\pi r/\lambda \equiv x$. The refractive index is $n_r = 1.33$, $n_i = 0$.

MOST RESONANCE FEATURES (OSCILLATIONS) DISAPPEAR WHEN A SIZE DISTRIBUTION IS USED (ALWAYS HAVE A RANGE OF SIZES IN NATURE)

PHASE FUNCTIONS

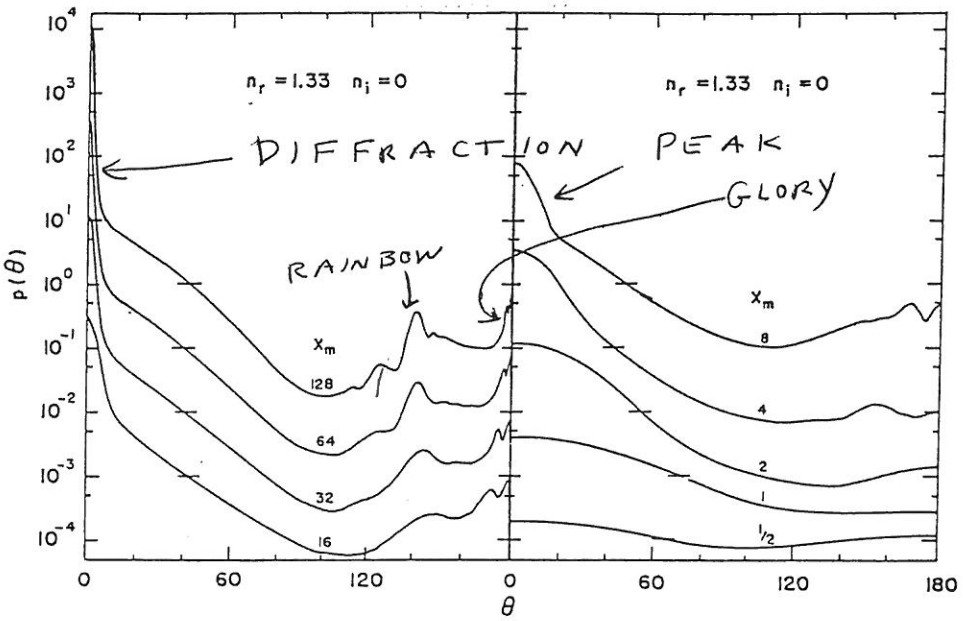

FIG. 1. Single-scattering phase functions for a size distribution of transparent spherical particles with a real refractive index typical of water and ice in the near infrared; the curves show the effect of changing the characteristic particle size. In Figs. 1–3 the vertical scales apply to the uppermost curve on the left side and the scales for the other curves may be obtained by multiplication by a power of 10 such that the horizontal bar on each curve occurs at $p(\theta) = 1$.

clouds often differ markedly from Deirmendjian's model, it serves the purpose of averaging out most of the large fluctuations which occur in the phase function (scattering diagram) for a single sphere. We have made preliminary computations to find the effect of changing the shape of the size distribution; the results for several different distributions indicate that the volume extinction (σ_{ext}), the single scattering albedo (ω), the asymmetry factor ($\langle\cos\theta\rangle$), and the shape of the phase function (oustide the region of the glory) depend mainly on

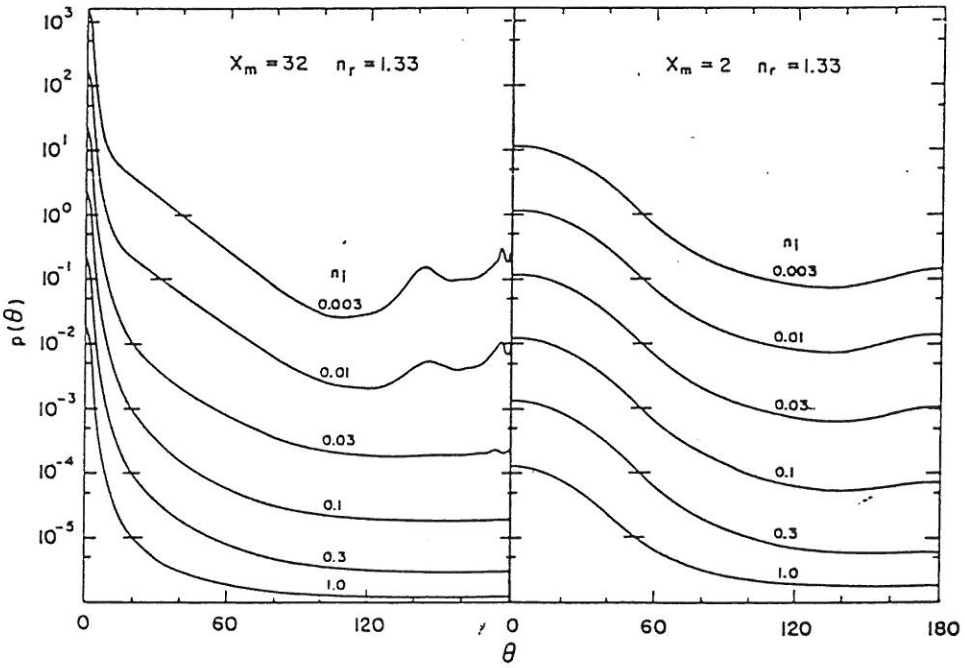

FIG. 2. Single-scattering phase functions for a size distribution of spherical particles showing the effect of absorption within the particles for large particles ($x_m = 32$) and particles of moderate size ($x_m = 2$).

NOTES ON PHASE FUNCTION:

(1) DIFFRACTION PEAK GETS NARROWER + HIGHER AS x INCREASES $\rightarrow$
WAY OF ESTIMATING PARTICLE SIZE

(2) RAINBOW (PRIMARY ONE)
IS RESONANCE FEATURE AT ANGLE OF MINIMUM DEVIATION FOR

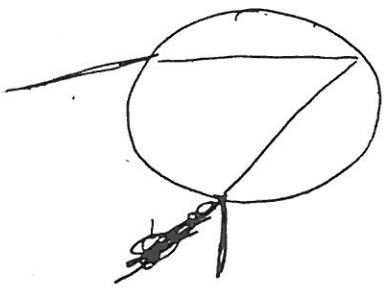

2 REFRACTIONS, 1 REFLECTION (INTERNAL)

RAINBOW Θ DEPEND ON m_r
SINCE $m_r(\lambda) \rightarrow$ VARIES W/ λ

(3) GLORY
ANOTHER RESONANT FEATURE AT BACKSCATTER ($\Theta = 180^\circ$)
(DUE TO CONSTRUCTIVE INTERFERENCE OF SURFACE WAVES)

SINGLE SCATTERING ALBEDO VS n_i

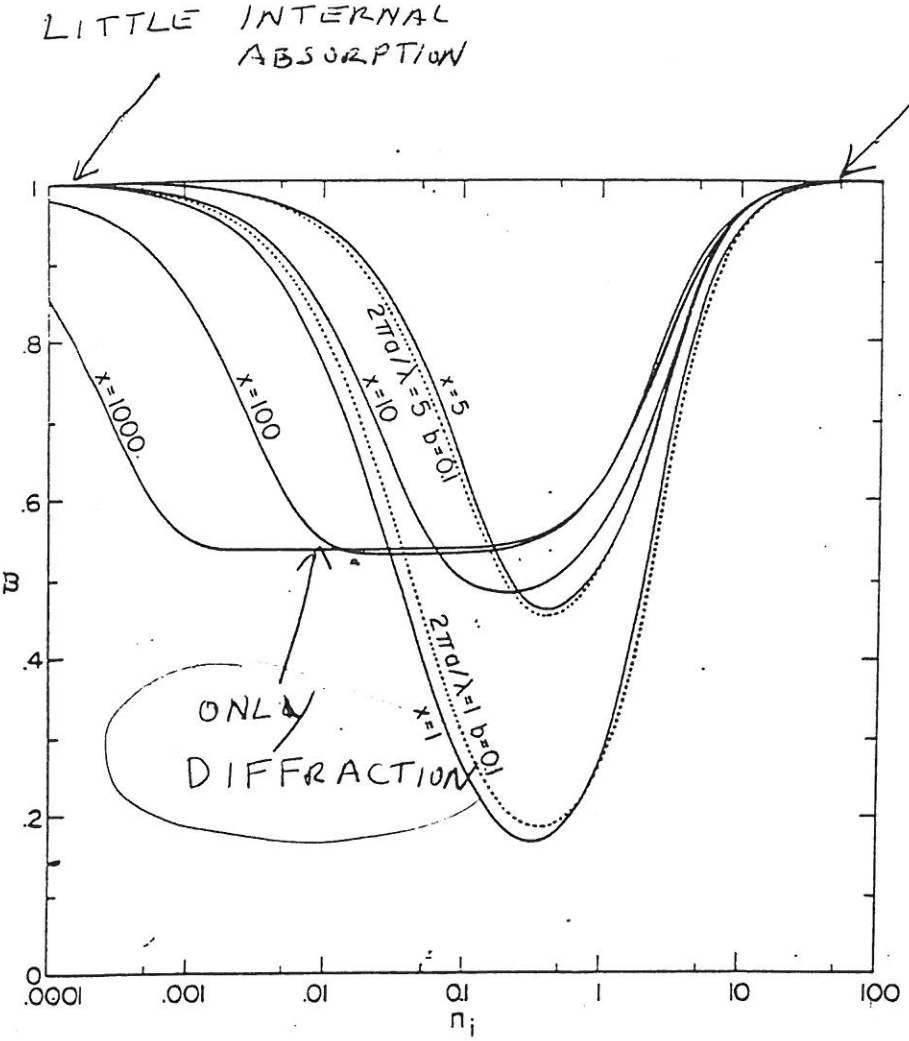

Fig. 10. Single scattering albedo, $\bar{\omega}$, as a function of the imaginary part of the refractive index, n_i. The solid curves are for $b=0$, corresponding to a single particle so $2\pi a/\lambda = 2\pi r/\lambda \equiv x$. The real refractive index is $n_r = 1.33$.

AS n_i ↑, AND AS x ↑, AMOUNT OF INTERNAL ABSORPTION ↑

INTERNAL ABSORPTION $\sim \exp(-k\ell) \sim \exp\left(-\frac{4\pi n_i}{\lambda} d\right)$

(k: absorption coefficient; ℓ: path length; d: diameter)

APPLICATION

REFLECTION SPECTRA OF SURFACES/CLOUD $\longrightarrow$ I/F $(\tilde{\omega}_0(\lambda))$

$\longrightarrow$ COMPOSITION, SIZE

$$\langle \cos \Theta \rangle = \int p \cos \Theta \frac{d\Omega}{4\pi}$$

USED IN 2 STREAM APPROXIMATIONS TO RT EQUATION

BIG PARTICLES PREFERENTIALLY SCATTER LIGHT INTO FORWARD HEMISPHERE

$\Theta < 90°$

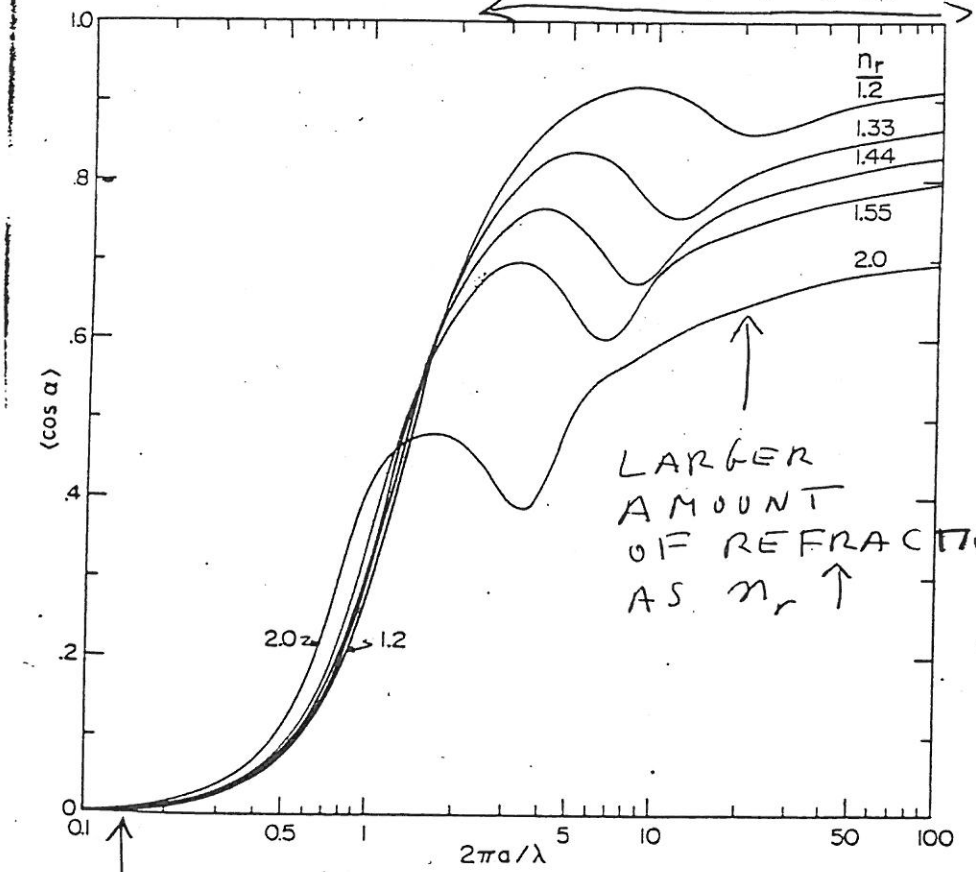

Fig. 12. Asymmetry parameter, ⟨cosα⟩, as a function of effective size parameter, $2\pi a/\lambda$. Results are shown for five values of the real refractive index, n_r, all with $n_i = 0$. The standard size distribution (2.56) was used with $b = 0.07$.

SMALL PARTICLES HAVE RAYLEIGH PHASE FUNCTION

USER HINTS ON MIE CALCULATIONS

- USE DEMIESS RATHER THAN DAMIE (DEMIESS MUCH FASTER)
  (DEMIESS FOR CORE/SHELL PARTICLES BUT SET CORE RADIUS = 10^{-10} SHELL R → HOMOGENEOUS CALCULATIONS)

- GRID SIZE IN (H) SHOULD BE FINER ~~[illegible]~~ AT SMALL (H) TO REPRESENT WELL THE DIFFRACTION PEAK

- IF ONLY WANT $\langle \cos\theta \rangle$ AND NOT P((H)) CAN GET Q, $\tilde{\omega}$, & $\langle \cos\theta \rangle$ FROM CALCULATIONS AT ONLY ONE (H)

- USE A SIZE DISTRIBUTION FUNCTION TO ELIMINATE MOST OSCILLATIONS

SIZE DISTRIBUTIONS

— ONLY 1ST 2 MOMENTS IMPORTANT

EFFECTIVE RADIUS, r_{eff}

$$r_{eff} = \int r\, Q\pi r^2 n(r)\,dr \Big/ \int Q\pi r^2 n(r)\,dr$$
$$\cong \int r\,\pi r^2 n(r)\,dr \Big/ \int \pi r^2 n(r)\,dr$$

EFFECTIVE VARIANCE, v_{eff} (WIDTH)

$$v_{eff} \cong \frac{\int (r - r_{eff})^2 \pi r^2 n(r)\,dr}{r_{eff}^2 \int \pi r^2 n(r)\,dr}$$

— COMMON DISTRIBUTIONS

(1) Hansen–Hovenier (GAMMA DISTR.)

$$n(r) = (\text{constant})\, r^{\alpha} \exp(-r/ab)$$
$$\alpha = (1-3b)/b$$
$$\longrightarrow \quad a = r_{eff}$$
$$b = v_{eff}$$

(2) Log Normal (COMMON IN NATURE)

$$n(r) = \frac{1}{(2\pi)^{1/2}} \frac{1}{\sigma_g r} \exp\left[-\frac{[\ln(r) - \ln(r_g)]^2}{2\sigma_g^2}\right]$$

$$r_g = r_{eff} / (1 + v_{eff})^{5/2}$$

$$\sigma_g^2 = \ln(1 + v_{eff})$$

HANSEN – HOVENIER

SIZE DISTRIBUTION

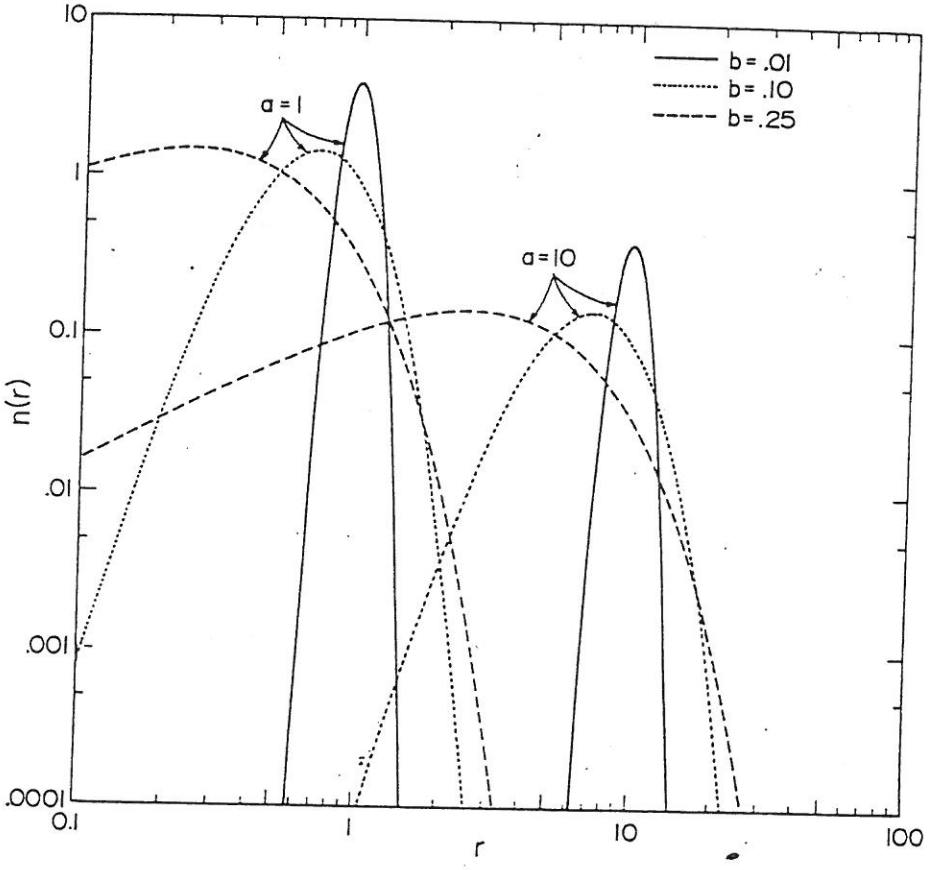

Fig. 7. Standard size distribution (2.56) for 2 values of a and three values of b. The size distributio is normalized so that the integral over all sizes is $N=1$.

The curve $b=0$ in Figure 8 gives Q_{sca} for a single particle, as a function of $x=2\pi r/\lambda$. This curve is characterized by a series of major maxima and minima of wavelengt ~10 in x and superimposed 'ripples' of wavelength ~0.8 in x. The major maxim and minima are due to interference of light diffracted ($l=0$) and transmitted ($l=1$ by the particle, these two components making up ~95% of the scattered light (Figur 4). The phase shift for a light ray passing through the sphere along a diameter i $\varrho=2x(n_r-1)$. Thus constructive (or destructive) interference occurs successively a intervals $\sim 2\pi$ in ϱ, or ~9.5 in x for $n_r=1.33$. The curves of Q_{sca} for other values o n_r are qualitatively similar if graphed as a function of ϱ, as shown in Figure 32 of van de Hulst (1957).

The ripple on the Q_{sca} curve for a single particle arises from the last few significant terms in the Mie series, (2.42), as demonstrated by Bryant and Cox (1966). According to the localization principle these terms arise from edge rays, i.e., from the light rays grazing the sphere. These rays set up surface electromagnetic waves which travel around the sphere spewing off energy in all directions. Since there are focal points at

=0° and $\alpha=180°$ the r
at $\alpha=180°$ the surface w
ne glory, and is the main
rom geometrical optics
o the intensity of diffra
rising from the surface
urve. van de Hulst (19
ogical models to explai
he surface waves are a
he model of Bryant an
lamped, i.e., that the
presented below for abs
he closer to reality.

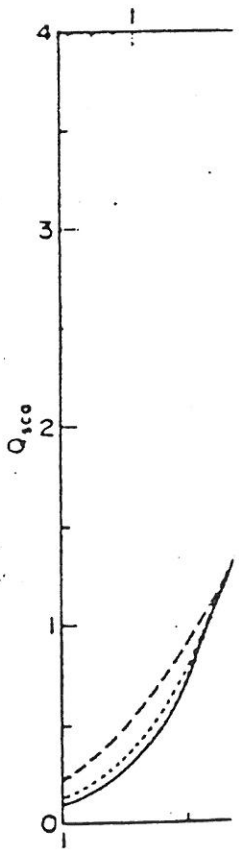

Fig. 8. Efficiency factor
standard size distribution
$b=0, 2$

COMPOSITE PARTICLES
(INCLUSIONS WITH A MATRIX)

It is not difficult to extend (8.49) or (8.47) to multicomponent mixtures. If we make the same assumptions for each inclusion that were made preceding (8.48), then the average dielectric function is

$$\epsilon_{av} = \frac{(1-f)\epsilon_m + \sum f_j \beta_j \epsilon_j}{1 - f + \sum f_j \beta_j},$$

ϵ_{av} = complex dielectric function = $\epsilon' + i\epsilon''$

AV = AVERAGE FOR COMPOSITE

m = matrix, j = species j INCLUSION

f_j = volume fraction occupied by species j

$f = \sum_j f_j$

(complex #) $\beta_j = 3\epsilon_m / (\epsilon + 2\epsilon_m)$ for spheres

$$\epsilon' = \frac{\varepsilon'}{\varepsilon_0} = n^2 - k^2,$$

$$\epsilon'' = \frac{\varepsilon''}{\varepsilon_0} = 2nk,$$

$$n = \sqrt{\frac{\sqrt{\epsilon'^2 + \epsilon''^2} + \epsilon'}{2}},$$

$$k = \sqrt{\frac{\sqrt{\epsilon'^2 + \epsilon''^2} - \epsilon'}{2}},$$

$n \longleftrightarrow n_r$ real index of refraction

$k \longleftrightarrow n_i$ imaginary index of refraction

SCATTERING BY NON-SPHERICAL PARTICLES (ie SOLIDS)

— IF SMALL, MIE THEORY IS GOOD APPROXIMATION
→ EQUAL VOLUME SPHERES

— IF BIG, USE:

— CLASSICAL DIFFRACTION THEORY

— EXTERNAL REFLECTION VIA ~~FRESNEL~~ FRESNEL EQ. FOR RANDOM ORIENTATIONS

— INTERNAL TRANSMISSION VIA EMPIRICAL EQ.

Q_{SCAT} → — FOR SCATTERING, USE EQUAL AREA SPHERE

Q_{abs} → — FOR ABSORPTION, USE EQUAL VOLUME SPHERE

EQUAL VOLUME SPHERE GIVE SIMILAR Q_{ext} TO NONSPHERES WHEN $X <$ few

FOR LARGER X, Q_{ext} (NON-SPHERES) > Q_{ext} (SPHERES)

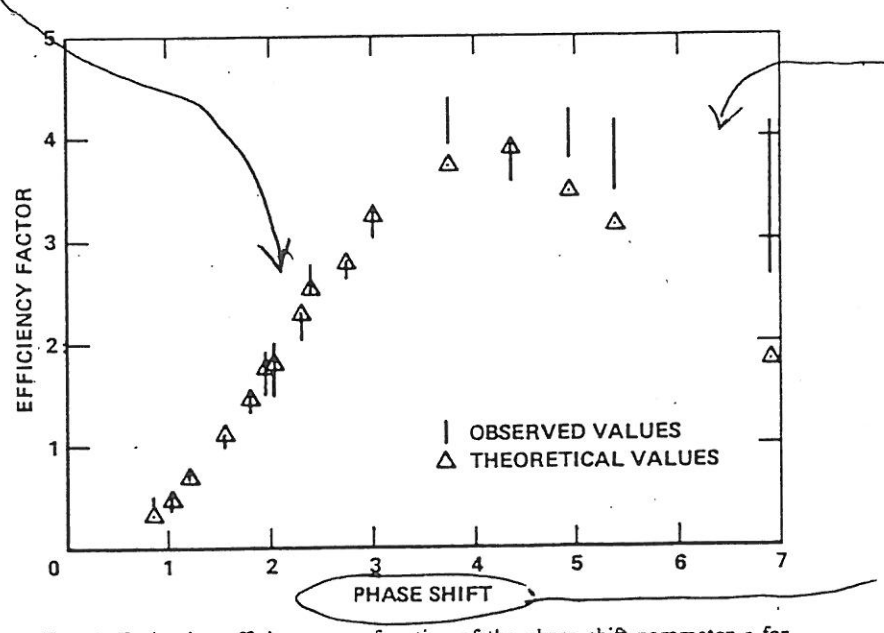

FIG. 1. Extinction efficiency as a function of the phase shift parameter ρ for particles composed of stacked cylinders. The vertical lines show these results for different orientations of the electric vector (Greenberg *et al.*, 1971). The triangles are the Mie scattering predictions for equal volume spheres having the same refractive indices. The phase shift parameter is defined by (1) in the text.

stacked cylinders (Greenberg *et al.*, 1971). The parameter ρ is defined by

$$\rho = 4\pi a_s(m_r - 1)/\lambda \equiv 2x(m_r - 1), \qquad (1)$$

where a_s, m_r, λ and x are, respectively, the radius of an *equal volume sphere*, real part of the index of refraction, wavelength, and size parameter or ratio of the equivalent sphere's circumference to the wavelength. The parameter ρ provides a measure of the phase shift experienced by an axial ray passing through the center of the particle. The vertical

PHASE FUNCTIONS OF EQUAL VOLUME SPHERES ≃ THOSE OF NON-SPHERES WHEN X ≤ few

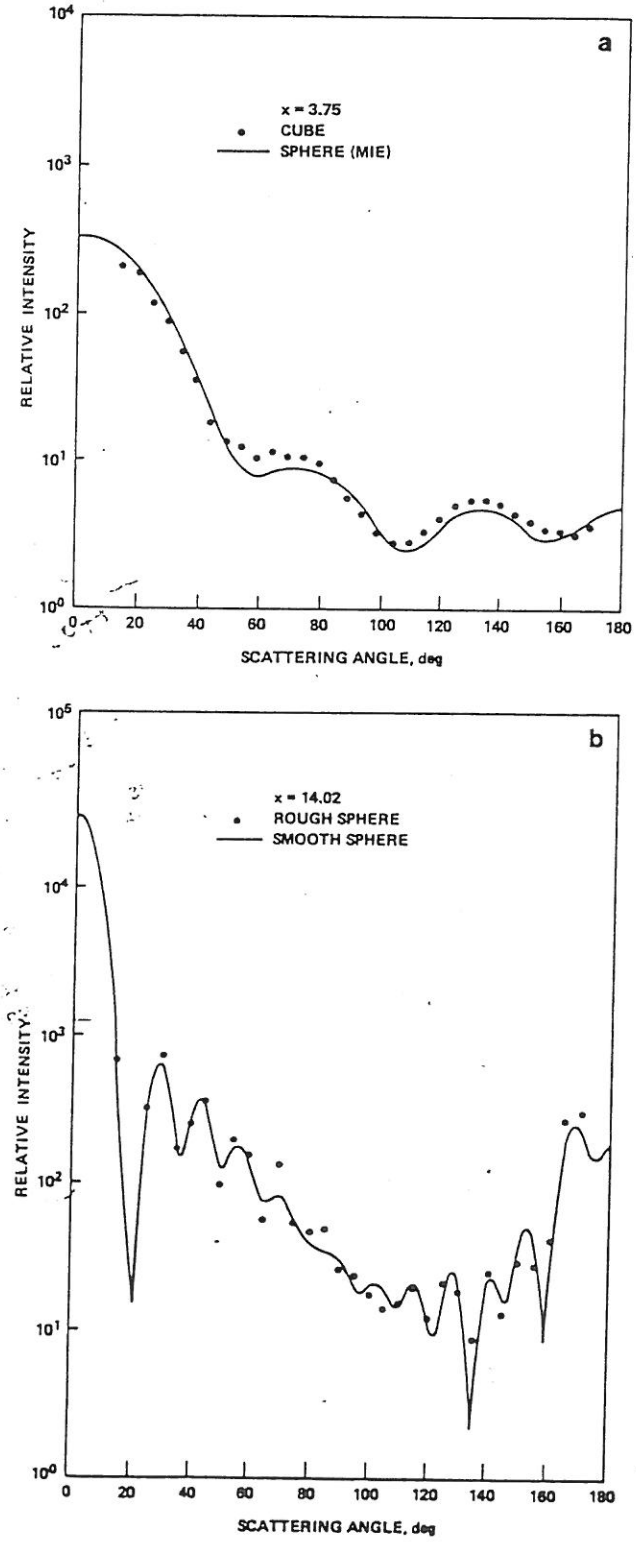

FIG. 2. Comparison of the angular distribution of scattered intensity obtained using analog techniques (dots) with Mie theory for an equal volume sphere having the same refractive index (solid line) (After Zerull and Giese, 1974). (a) A small cube, (b) a corrugated sphere. For these cases, $\tilde{m} = 1.57 - 0.006i$ and hence $\rho = 1.14x$.

Several conclusions can be drawn from Fig. 1. First, for $\rho \leqslant 4$, the stacked cylinders have about the same dependence of Q_{ext} on ρ as do equal volume spheres. Second, for $\rho > 4$, Q_{ext} is systematically higher than the value appropriate for the equivalent sphere. This disagreement is not unexpected and can be understood in the following way: In the limit of $\rho \gg 1$, the total cross section of an arbitrarily shaped particle tends asymptotically toward twice its physical cross section (van de Hulst, 1957). Recalling that Q_{ext}, as given in Fig. 1, is defined as the ratio of the total cross section to the physical cross section of an *equal-volume sphere*, we expect that Q_{ext} will tend toward $2(A_{lr}/A_{sphere})$ for a randomly oriented, large, irregular object, where A_{lr} and A_{sphere} are the projected surface areas of the irregular object and an equal volume sphere, respectively. Note that had we defined Q_{ext} as equal to the ratio of the total cross section to the physical cross section of the irregular particle, Q_{ext} would approach 2. Over the gamut of particle shapes, a sphere has the smallest ratio of surface area to volume. Hence $A_{lr} > A_{sphere}$ and $Q_{ext} > 2$.

Other laboratory measurements on irregular particles support the above conclusions and provide some further information. Berry (1962) studied the extinction characteristics of randomly oriented, monodisperse cubes of silver bromide at visible wavelengths. These measurements showed that, in the Rayleigh domain $\rho \leqslant 1$, Q_{ext} is quite close to that expected for equal volume spheres. Also, at larger values of ρ, Q_{ext} for the cubes displayed a resonant structure similar to that of spheres, although the primary maximum appeared to occur at a somewhat larger value of ρ than that expected for an equal volume sphere. This latter result is supported by Proctor and Barker's (1974) and Proctor and Harris' (1974) visible-wavelength studies of randomly oriented polydispersed samples of irregularly shaped diamond and quartz particles, respectively, as well as the microwave measurements of Greenberg *et al.* (1961) on prolate spheroids. Proctor and Harris also found that the extinction efficiency had an almost constant value for $\rho > 10$, i.e., in this domain it closely approached the asymptotic value appropriate for geometrical optics.

Not only do randomly oriented, irregular particles have approximately the same cross section as that of equal volume spheres when $\rho \leqslant$ some critical value $\rho_0 \approx$ several, but there also appears to be a similar equivalence for the angular dependence of the scattered intensity, the phase function (Zerull and Giese, 1974). This deduction is illustrated in Figs. 2a and 2b for small, randomly oriented cubes and corrugated spheres, respectively (*ibid.*). The dots show the measured phase function, while the solid lines show the predicted Mie behavior.

When $\rho > \rho_0$, nonspherical particles show marked

LARGE PARTICLE PRESCRIPTIONS

DIFFRACTION

Bessel function

$$d(\tilde{x}) = C_D \frac{(\tilde{x})^2}{4\pi}\left[\frac{2J_1(z)}{z}\right]^2 k$$

$$\approx \frac{2C_D \sin^2(\tilde{x}\sin\theta - \pi/4)k}{\pi^2\tilde{x}\sin^3\theta}, \qquad (2a)$$

where

$$z = \tilde{x}\sin\theta = \frac{2\pi\tilde{a}}{\lambda}\sin\theta, \qquad (2b)$$

$$k = \tfrac{1}{2}(1 + \cos^2\theta). \qquad (2c)$$

The phase function for diffraction is then given by

$$I_D = \int_{x_0}^{\infty} d(\tilde{x})\pi\tilde{x}^2 n(\tilde{x})\,d\tilde{x}, \qquad (2d)$$

where $n(\tilde{x})$ is the size distribution of interest and C_D is obtained from the usual normalization condition

$$\int I_D \frac{d\Omega}{4\pi} = 1. \qquad (2e)$$

$$Q_{DIFF}(\tilde{x}) = r = \frac{\text{Surface Area (nonsphere)}}{\text{Surface Area (= vol. sphere)}}$$

EXTERNAL REFLECTION

$$I_R = \tfrac{1}{2}C_R\left\{\frac{\sin(\theta/2) - [|\tilde{m}|^2 - 1 + \sin^2(\theta/2)]^{1/2}}{\sin(\theta/2) + [|\tilde{m}|^2 - 1 + \sin^2(\theta/2)]^{1/2}}\right\}^2$$

$$+ \tfrac{1}{2}C_R\left\{\frac{|\tilde{m}|^2\sin(\theta/2) - [|\tilde{m}|^2 - 1 + \sin^2(\theta/2)]^{1/2}}{|\tilde{m}|^2\sin(\theta/2) + [|\tilde{m}|^2 - 1 + \sin^2(\theta/2)]^{1/2}}\right\}^2, \qquad (3a)$$

where

$$|\tilde{m}|^2 = m_r^2 + m_i^2 \qquad (3b)$$

and C_R is found from

$$\int I_R \frac{d\Omega}{4\pi} = 1. \qquad (3c)$$

$$Q_{refl.}(\tilde{x}) = \frac{r}{C_R}$$

INTERNAL TRANSMISSION

VERY SENSITIVE TO SHAPE!

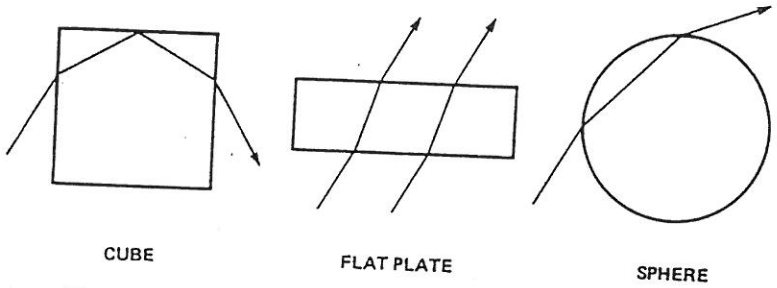

FIG. 5. Paths of light rays through a cube, a flat plate and a sphere.

$$I_{Tran} = C_T \exp\left(1 + b\,\textcircled{H} + c\,\textcircled{H}^2\right)$$

C_T found from:

$$\int I_T \frac{d\Omega}{4\pi} = 1$$

Forward to Back hemisphere ratio, G

$$G \equiv \int_0^{\pi/2} I_T\, d\textcircled{H} \Big/ \int_{\pi/2}^{\pi} I_T\, d\textcircled{H}$$

Quadratic Term allows for a backscatter ($\textcircled{H} = 180°$) PEAK

$$Q_T(\hat{x}) = Q_{EXT}^{Large} - Q_{DIFF} - Q_{REFL}$$

deviations in their phase functions from that of their spherical counterparts, especially at intermediate and large angles of scatter. This point is illustrated in Figs. 3 and 4, which display measurements for randomly oriented cubes (Zerull and Giese, 1974) and flat flakes (Holland and Gagne, 1970), respectively. In these figures the dots and vertical bars indicate the observed values and their associated error bars, while the dashed and dotted lines indicate the Mie predictions for equal volume spheres and equal area spheres, respectively. The solid line in each figure is discussed later. In both figures, resonant features, such as the Mie backscatter peak, are absent for the nonspherical particles. Thus, in the backscatter direction, the Mie curves lie above the observed ones, while at intermediate angles of scatter, the converse is true. We also note that at those angles where there is a sizeable departure from Mie scattering behavior, the logarithm of the phase function varies approximately linearly with scattering angle.

Figs. 3 and 4 also imply that Mie scattering theory provides an approximate fit to the measurements at small angles of scatter. Further evidence for this proposition is given by the visible light scattering experiments of Hodkinson (1963) and Ellison (1957).

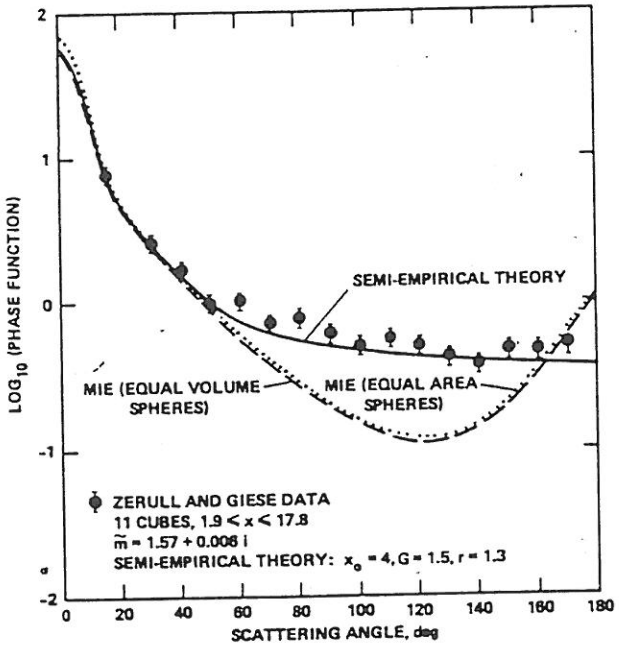

FIG. 3. Comparison of the phase function for scattering by a distribution of various sized cubes (dots with error bars), as obtained by numerically integrating results from analog measurements (Zerull and Giese, 1974), with the predictions of Mie theory for equal volume and equal area spheres and the semi-empirical theory of this paper. Each theoretical curve has been normalized to its correct vertical position with respect to the data points. Consequently, the normalization convention differs slightly among the three theoretical curves.

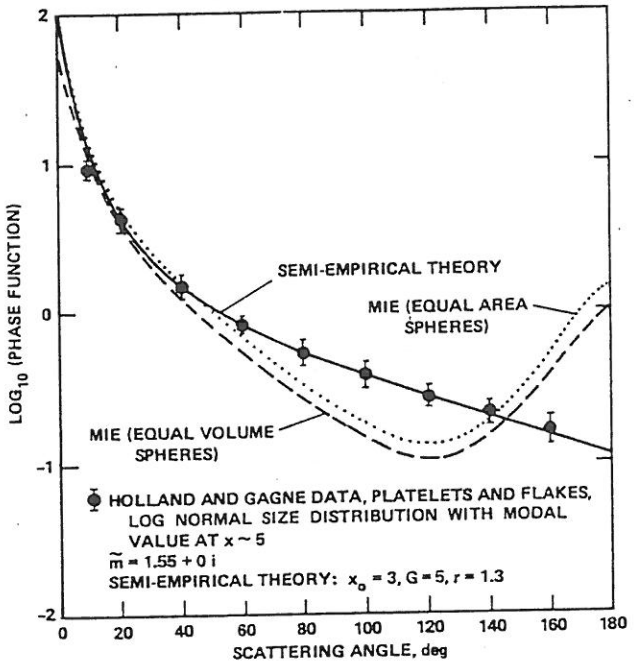

FIG. 4. Comparison of the measured phase function for scattering by an ensemble of flat plates, dots with error bars (Holland and Gagne, 1970), with the predictions of Mie theory for equal volume and equal area spheres and the semi-empirical theory of this paper. A value of $r = 2.0$ yields a virtually identical result for the semi-empirical phase function.

Hodkinson compared the scattering behavior of large quartz and flint particles having almost the same index of refraction and size distribution. Although the flint particles appeared much more irregular under microscopic examination, the two sets of material exhibited almost identical scattering diagrams at small scattering angles ($\leq 60°$). Hodkinson also showed that at small scattering angles, the measured phase function of large quartz and diamond particles ($x \sim 10$–100) were very similar to those of *equal area* spheres. The phase function of the latter was approximated by the sum of the diffraction pattern of an opaque disk of equal projected area and the external reflection and internal refraction components calculated according to geometrical optics theory. Hodkinson and Greenleaves (1963) had previously shown that this recipe gave a good fit to Mie theory results at small scattering angles.

Finally, Ellison (1957) measured the extinction efficiency of randomly oriented silica dust ($x \sim 10$–100) with a detector whose acceptance angle included the light scattered at small scattering angles. He showed that a prescription similar to that of Hodkinson gave predictions for the fraction of the scattered beam within his acceptance angle which were consistent with the observed dependence of the measured efficiency on x.

TABLE 1. Model parameters derived from laboratory measurements.

Data[a]	$\bar{m}$[b]	x_0[c]	G[c]	$\langle\cos\theta\rangle$[d]	$\langle\cos\theta\rangle$[d] (equivalent spheres)
Large cubes					
$x = 5.9–17.8$					
$n(x) = n_0 x^{-4}$	$1.57 + 0.006i$	4	1.5 to 2.0	0.540	0.672
All cubes					
$x = 1.9–17.8$					
$n(x) = n_0 x^{-2.5}$	$1.57 + 0.006i$	4	1.5 to 2.0	0.560	0.690
All cubes					
$x = 1.9–17.8$					
$n(x) = n_0 x^{-2.5}$	$1.70 + 0.015i$	2	1.5	0.482	0.681
Octahedra					
$x = 5.9–9.1$					
$n(x) = n_0 x^{-2.5}$	$1.50 + 0.005i$	7–8	2	0.520	0.570
Convex-concave					
$x = 5.9–17.8$					
$n(x) = n_0 x^{-2.5}$	$1.50 + 0.005i$	10	3 to 4	0.601	0.719
Flat plates or flakes					
$x = 2–20$					
log-normal	1.57 to $0i$	3	5	0.600	0.675

[a] The measurements on the cubes, octahedra and convex-concave particles were made by Zerull and Giese (1974) and Zerull (1976), while those for the flat flakes were obtained by Holland and Gagne (1970). In the case of the convex-concave particles, we used an average of the separate measurements made on convex and concave particles. The information given in this column includes the range of x values covered by the measurements and the size distribution $n(x)$ within this range.

[b] $\bar{m}$ is the complex index of refraction.

[c] x_0 and G are parameters of the nonspherical particle scattering theory, which were derived by matching the measurements cited in the leftmost column. In the case of the cubes and the convex-concave particles, the parameter r was estimated to be ~1.3, while it was found to be ~1.1 for the octahedra. For the flakes, the value of r may not be accurately obtained due to the choice of equal *area* spheres as reference material and the relatively small contribution of the particles with $x < x_0$ (see Section 3c). Values of 1.3 and 2.0 both provide virtually identical results. From strictly geometrical considerations, r should equal 1.3 for cubes and about 1.1 for octahedra. The parameters x_0, G and r are defined in the text.

[d] See Eq. (9).

the data and hence represent close to optimum but not necessarily the optimum numbers. Further refinements to the fit do not appear to us to be warranted by the state of either the theory or the data. The joint influence of the small- and large-size regime is nicely illustrated in Fig. 7. For this case, x_0 has a value close to the midpoint of the range of x values included in the size distribution function. The rise of the phase function in the backscattering direction is due to the backscattering resonances present in the small-size regime, while departures of the observed phase function from the one predicted by Mie theory at intermediate and large angles is due to the influence of particles in the large-size regime and, in particular, to their transmission component.

4. Discussion

The relatively simple structure of our theory provides insight into the similarities and differences in the scattering behavior of irregular particles and that of their equal volume spherical counterparts. First, according to our theory, polydispersed ensembles of *small* irregular particles, i.e., $x < x_0$ for all particles, are expected to exhibit essentially the same scalar scattering behavior as that of their equivalent volume spheres. However, as discussed in Section 3a, such an equality in behavior breaks down for elongated particles having large $|\bar{m}|$, with such particles having higher cross sections than their spherical counterparts.

Next, we consider an ensemble of large irregular particles, i.e., $x > x_0$ for all particles. According to (7a), the average *scattering* efficiency of such particles differs from that of equal volume spheres only by a factor equal to the ratio of their surface areas r. This parameter is a weak function of particle shape. But, when $2m_i x < 1$, the usual situation, the *absorption* efficiency of the irregular particles is the same as that for their spherical counterparts, according to (7b). In this case, the single-scattering albedo of the irregular particles is somewhat higher than that of the equivalent spheres.

The *shape* of the phase function at small scattering angles is determined primarily by diffraction and external reflection. Therefore, it is not significantly affected by particle irregularity, except for a factor of $(r)^{1/2}$ by which the radius of the equal volume spheres must be multiplied in the computation of the diffraction pattern.

The main deviation in the scattering behavior of

SUGGESTED READING

(1) RM Goody & YL Yung, "Atmospheric Radiation, Theoretical basis" 2nd ed, Oxford Univ. Press, ~~Chapt~~ Chapter 7

(2) C. F. Bohren & DR Huffman, "Absorption and Scattering of Light by Small Particles" John Wiley, 1983

(3) JB Pollack & JN Cuzzi, "Scattering by nonspherical particles of size comparable to a wavelength", J. Atmospheric Sci., 37, 868-881

(4) JE Hansen & LD Travis, "Light Scattering in Planetary Atmospheres", Space Sci. Rev., 16, 527-610, 1974